ChemComm

COMMUNICATION

View Article Online
View Journal | View Issue

Cite this: *Chem. Commun.*, 2024, **60**, 2393

Received 7th November 2023,
Accepted 26th January 2024

DOI: 10.1039/d3cc05482a

rsc.li/chemcomm

Heterobifunctional rotaxanes featuring two chiral subunits – synthesis and application in asymmetric organocatalysis†

Dana Kauerhof, Jan Riebe, Christoph J. Vonnemann, ‡ Maike Thiele, Dennis Jansen and Jochen Niemeyer *

Rotaxanes can serve as scaffolds for the generation of bifunctional catalysts. We have now generated acid–base functionalized rotaxanes featuring two chiral subunits. The mechanical bond leads to increased reaction rates and also to strongly altered enantioselectivites in comparison to the non-interlocked control catalysts.

Mechanically interlocked molecules (MIMs),[1] such as catenanes and rotaxanes, have found increasing attention for the design of novel catalysts.[2] Here, the mechanical bond offers exciting possibilities for catalyst design based on the flexible, but permanent connection of two or more subunits. For example, MIMs can provide unique three-dimensional environments around a catalytically active site.[3] The possibility to control the co-conformation of MIMs has been used to create switchable catalysts, including ON/OFF switchability but also a switchability between different reaction modes.[4] Furthermore, MIMs allow for the generation of bi- or multifunctional systems by introduction of several functional groups on the subcomponents.[5] Last but not least, the mechanical bond can be used for the introduction of chirality:[6] achiral subcomponents of suitable symmetry can be interlocked to give MIMs with nonclassical mechanical chirality.[7,8] Alternatively, chiral subcomponents can be used, *e.g.* in order to transfer the chiral information *via* the mechanical bond (Fig. 1).[9]

Berna, Leigh and Takata have previously reported chiral interlocked catalysts that feature either chiral macrocycles or chiral threads (Fig. 1a–d). In our group, homobifunctional catenanes composed of two chiral macrocycles with 1,1′-binaphthyl phosphoric acids were used in enantioselective transfer hydrogenations (Fig. 1e).[10] Furthermore, heterobifunctional rotaxanes composed of a macrocycle with a chiral 1,1′-binaphthyl phosphate and an achiral dibenzyl-ammonium-thread were used as catalysts for enantioselective Michael-

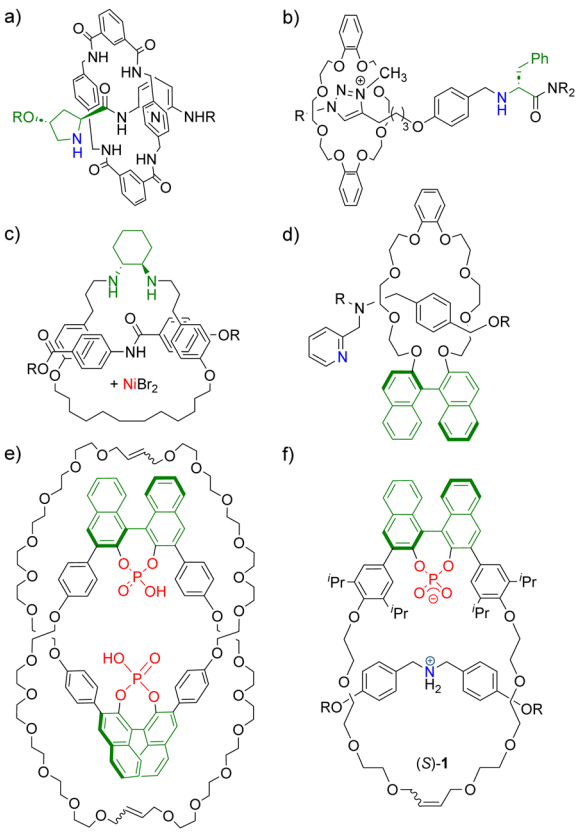

Fig. 1 Previously reported interlocked catalysts featuring chiral threads or macrocycles from Berna (a),[9a] Leigh (b) and (c),[9d,e] Takata (d)[9c] and Niemeyer (e) and (f).[10,11] Chiral units shown in green, catalytically active centers shown in blue/red. Examples of previously reported interlocked catalysts from ref. 9*b* and *f* not shown.

Faculty of Chemistry (Organic Chemistry) and Centre of Nanointegration Duisburg-Essen (CENIDE), University of Duisburg-Essen, Universitätsstr. 7, 45141 Essen, Germany. E-mail: jochen.niemeyer@uni-due.de

† Electronic supplementary information (ESI) available: Syntheses and analytical data for all catalysts, details of catalytic reactions. See DOI: https://doi.org/10.1039/d3cc05482a

‡ Current address: Faculty of Chemistry and Biochemistry, Organic Chemistry I, Ruhr-Universität Bochum, Universitätsstraße 150, 44801 Bochum, Germany.

additions (*e.g.* rotaxane (*S*)-**1**, Fig. 1f).[11] Both for the catenanes and the rotaxanes, we found that the interlocked catalysts can deliver enhanced stereoselectivities in comparison to their non-interlocked counterparts. For the rotaxane-catalysts, we also found increased reaction rates.

Supported by extensive DFT-calculations, the increased rates and selectivities were attributed to a cooperativity between the functional groups, enabled by the mechanical bond, demonstrating the power of using MIMs as catalysts.[11]

However, the use of multiple elements of chirality in MIM-based catalysts has not been investigated to the best of our knowledge. Herein, we report the synthesis and catalytic application of rotaxanes featuring both a chiral macrocycle and a chiral thread. Based on our previously reported rotaxane (*S*)-**1** (Fig. 1f), we developed two novel rotaxanes: These contain the same 1,1′-binaphthyl phosphate macrocycle, but now feature a chiral thread either based on Maruokas 1,1′-binaphthyl azepine[12] or based on 3-hydroxy-prolinol. For a first investigation of their catalytic performance, we only generated one diastereomer of each rotaxane.

The rotaxanes were generated by a CuAAc-based stoppering approach, using our previously established phosphate-ammonium passive template.[11] The required ammonium-bisalkynes were synthesized as follows (Fig. 2): Starting from 3,3′-diiodinated azepine (*S*)-**4** (available in 8 steps from BINOL[13]), bisalkyne (*S*)-**5** was synthesized by Suzuki-coupling with 4-hydroxyphenylboronic acid, followed by propargylation, Boc-deprotection and anion-exchange (45% yield over three steps). Starting from commercially available Boc-protected 3-hydroxy-prolinol (*R*,*S*)-**6**, bisalkyne (*R*,*S*)-**7** was generated by propargylation and Boc-deprotection plus anion-exchange (55% yield over two steps). To generate the rotaxanes, the 1,1′-binaphthyl phosphate based macrocycle (*S*)-**8**[11] was reacted with bisalkyne (*S*)-**5** or (*R*,*S*)-**7** and stopper-azide **9**[11] to give either the azepin-based rotaxane (*S*,*S*)-**2** or the hydroxyprolinol-based rotaxane (*S*,*R*,*S*)-**3** (Fig. 2). The rotaxanes were isolated as the zwitterionic phosphate-ammonium-salts and obtained in yields of 20/37%. Due to the C_2-symmetry of the phosphate-macrocycle, no orientational isomers are expected for these rotaxanes.

All precursors, threads (independently synthesized) and rotaxanes were fully characterized by standard analytical methods and the purity of the final catalyts was further demonstrated by HPLC-analyses (ESI,† Fig. S18, S29 and S32). Here, we will briefly discuss rotaxane (*S*,*R*,*S*)-**3**: In the NMR (Fig. 3), the interlocking of both subcomponents leads to distinct changes in chemical shifts, *e.g.* for the olefinic unit of the macrocycle (δ = 5.63 *vs.* 5.76 ppm for rotaxane *vs.* free macrocylce) and the ammonium-group on the thread (δ = 9.76 + 8.67 *vs.* 5.36 ppm for rotaxane *vs.* free thread).

The strong downfield shift of the NH_2^+-group is indicative of the mechanointramolecular phosphate-ammonium interaction. By high-resolution mass-spectrometry, the rotaxane can unambiguously be identified as the [M + 2H]-dication at *m*/*z* = 1253.0875 (calculated *m*/*z* = 1253.0981).

With both rotaxanes in hand, we tested their application in asymmetric catalysis of the Michael-addition of diethylmalonate **11** to cinnamaldehyde **10a**. Based on our previously established protocol, the inactive ammonium-phosphate rotaxanes were first deprotonated by LiOH[14] to give the active catalysts in the $(ArO)_2POOLi\cdots HNR_2$ form. The reaction was carried out in tetrahydrofurane-d_8 and followed by NMR over 7

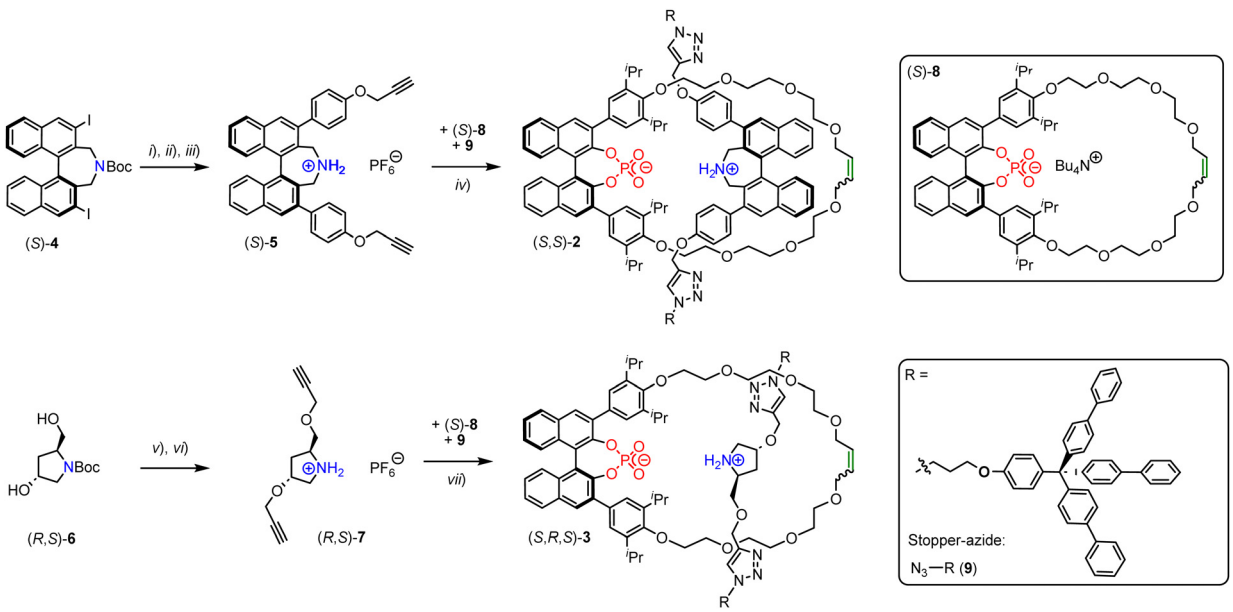

Fig. 2 Synthesis of rotaxanes (*S*,*S*)-**2** and (*S*,*R*,*S*)-**3**. Reagents and conditions: (i) 4-hydroxyphenylboronic acid, $Pd(PPh_3)_4$, 2 M Na_2CO_3 (aq.), DME, 90 °C, 2 h, 81%; (ii) propargyl bromide, cesium carbonate, DMF, 1.5 h, 68% (iii) trifluoroacetic acid, DCM, r.t., 2 h, then NaOH, then hydrochloric acid/dioxane, Et_2O, r.t., 30 min, then ammonium hexafluorophosphate, DCM, r.t., 16 h, 81%; (iv) $[Cu(MeCN)_4PF_6]$, CH_2Cl_2, r.t., 4 h, 20%; (v) propargyl bromide, sodium hydride, THF, r.t. 16 h, 70%; (vi), trifluoroacetic acid, DCM, r.t., 16 h, then NaOH, then hydrochloric acid/dioxane, Et_2O, r.t., 30 min, then ammonium hexafluorophosphate, DCM, r.t., 16 h, 79%; (vii) $[Cu(MeCN)_4PF_6]$, CH_2Cl_2, r.t., 4 h, 37%.

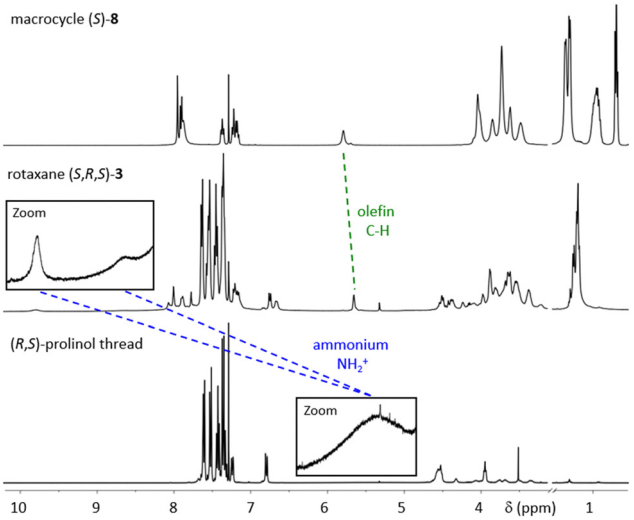

Fig. 3 ^{1}H NMR spectra of macrocycle (*S*)-8, rotaxane (*S*,*R*,*S*)-3 and (*R*,*S*)-prolinol-thread (all: $CDCl_3$, 400 MHz, 298 K).

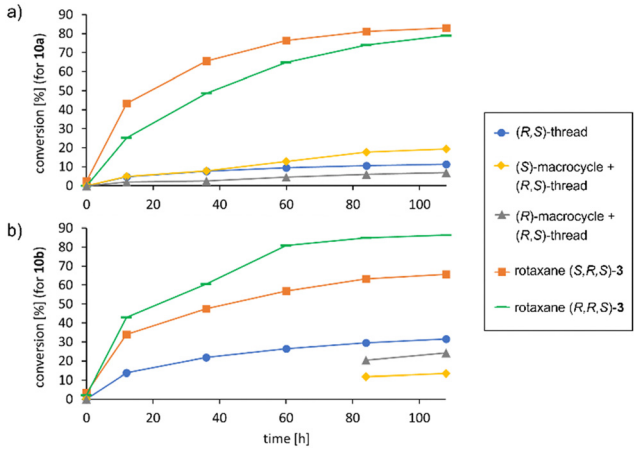

Fig. 4 Conversion curves for the addition of diethyl malonate to cinnamaldehyde **10a** (a) or its naphthyl-derivative **10b** (b, first four data points missing for non-interlocked mixtures) catalyzed by rotaxanes **3** or their non-interlocked subcomponents.

days, followed by isolation and analysis of the products. Surprisingly, no conversion was found for the azepine-based rotaxane (*S*,*S*)-**2**, while the prolinol-based rotaxane (*S*,*R*,*S*)-**3** gave 84% conversion after 7 days. This might be attributed to the higher basicity of the prolinol-unit in comparison of the dibenzoazepine (*cf.*, pK_a = 11.3 for pyrrolidinium, pK_a = 8.5 for dibenzylammonium), according to the role of the amine as a Brønsted-base in the catalytic mechanism.[11]

Due to the inactivity of rotaxane **2**, we decided to investigate only the prolinol-based system **3** in more detail. To obtain a full picture about the influence of the chiral subcomponents on the behaviour in catalysis, we also synthesized the diastereomeric rotaxane (*R*,*R*,*S*)-**3**, which features the same (*R*,*S*)-prolinol-based thread, but now in combination with the (*R*)-configured macrocycle (for synthetic details and full characterization of (*R*,*R*,*S*)-**3** and the (*R*,*S*)-prolinol thread, see the ESI,† Section 2.3).

In the application in catalysis, both rotaxanes were compared to the free (*R*,*S*)-prolinol thread and the non-interlocked mixtures of (*R*,*S*)-thread with either (*S*)- or (*R*)-macrocycle.[15] To further extend the scope of this investigation, we used both cinnamaldehyde **10a** and its naphthyl-derivative **10b** as electrophiles in the Michael-addition reaction. Interestingly, **10b** has not been previously described as an electrophile for malonate addition. When generating the racemic reference product (*rac*)-**12b**, we found a complex product mixture under standard conditions (diethylmalonate nucleophile, pyrrolidine catalyst), and only when using a lithium-phosphate + dibenzylamine catalysts, the product could be obtained.

To our delight, the rotaxane-catalysts **3** cleanly convert both substrates **10a/b** into the corresponding products **12a/b**. Here, the rotaxanes are significantly more active (71–84% conversion after 7 days) than the thread alone (12–34% conversion) or the non-interlocked mixtures of subcomponents (7–30% conversion) (Fig. 4 shows the first 5 days). This is in line with our earlier findings for rotaxane (*S*)-**1**, which showed that the interlocked nature of the catalyst results in cooperative behaviour of the lithium-phosphate and the amine group, leading to increased reaction rates.

However, to our surprise, the incorporation of the chiral prolinol-thread did not lead to an increase in stereoselectivity. While we did observe matched/mismatched effects for the diastereomeric rotaxanes (*S*,*R*,*S*)-**3** and (*R*,*R*,*S*)-**3** both for **12a** (−8%/29% ee) and the naphthyl-derivative **12b** (−30%/0% ee), the overall stereoselectivities were not higher than those observed for our reference rotaxane (*S*)-**1** (53%/29% ee for **12a/b**), which features the same chiral macrocycle, but an achiral thread. When comparing the rotaxanes to their non-interlocked counterparts (thread or macrocycle + thread), the following trends can be observed: Firstly, the (*R*,*S*)-prolinol thread alone only gives poor enantioinduction (14%/11% ee for **12a/b**). When combining the thread with the (*R*)-macrocycle, enantioselectivities remain largely unchanged for the non-interlocked mixture (21%/15% ee for **12a/b**), but show slightly stronger changes when mechanically interlocked in rotaxane (*R*,*R*,*S*)-**3** (29%/0% ee for **12a/b**). When combining the thread with the (*S*)-macrocycle, the stereoselectivities of the non-interlocked mixture (36%/18% ee for **12a/b**) are actually inverted in comparison to the rotaxane (*S*,*R*,*S*)-**3** for both substrates (−8%/−30% ee for **12a/b**). Thus, although absolute enantioselectivies remain low due to the inversion of the preferred product configuration, the mechanical bond does lead to strong relative changes in enantioselectivity in case of the (*S*)-macrocycle (Δee = 44–48%, *i.e.* $\Delta\Delta G^{\neq}$ = 0.48–0.54 kcal mol^{-1}) between interlocked and non-interlocked catalyst (Table 1).

In conclusion, we could demonstrate the synthesis and application of rotaxane-organocatalysts featuring two chiral subunits. While an azepine-based rotaxane was inactive, the use of a prolinol-thread gave rise to active organocatalysts for the asymmetric Michael-addition of malonates to α,β-unsaturated aldehydes. We could show that for two different substrates, the rotaxanes show significantly increased reaction rates in comparison to their non-interlocked counterparts,

Table 1 Catalytic results for rotaxanes (*S*)-**1**, (*S*,*R*,*S*)-**3** and (*R*,*R*,*S*)-**3**, their corresponding amine-threads and the non-interlocked mixtures of threads and macrocycles

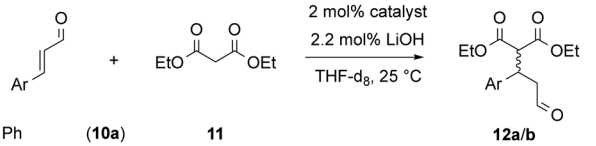

Ar = Ph (**10a**) **11** **12a/b**
Ar = 1-naphthyl (**10b**)

Entry	Catalyst precursor	Substrate	Conversion[a] (%)	ee[bc] (%)
1	Rotaxane (*S*)-**1**[d]	**10a**	88	53
2	(*S*)-Macrocycle + achiral thread[d]	**10a**	76	9
3	(*R*,*S*)-Prolinol-thread	**10a**	12[e]	17
4	(*S*)-Macrocycle + (*R*,*S*)-thread	**10a**	30	37
5	Rotaxane (*S*,*R*,*S*)-**3**	**10a**	84	−8
6	(*R*)-Macrocycle + (*R*,*S*)-thread	**10a**	7[e]	21
7	Rotaxane (*R*,*R*,*S*)-**3**	**10a**	82	30
8	Rotaxane (*S*)-**1**	**10b**	54	32
9	(*S*)-Macrocycle + achiral thread	**10b**	11	5
10	(*R*,*S*)-Prolinol-thread	**10b**	34	10
11	(*S*)-Macrocycle + (*R*,*S*)-thread	**10b**	18	16
12	Rotaxane (*S*,*R*,*S*)-**3**	**10b**	71	−30
13	(*R*)-Macrocycle + (*R*,*S*)-thread	**10b**	30	17
14	Rotaxane (*R*,*R*,*S*)-**3**	**10b**	82[e]	0

[a] Determined by ^{1}H NMR after 7 days. [b] Determined by chiral HPLC for isolated products. [c] Positive ee denotes excess of the (*R*)-isomer, according to assignment of HPLC-peaks in ref. 16. [d] Data taken from ref. 11. [e] After 5 days.

indicating a cooperative behaviour of the functional groups, enabled by the mechanical bond. The observed stereoselectivities were moderate, but a strong difference between the interlocked rotaxanes and the non-interlocked control catalysts (Δee = 44–48%) also demonstrates the effect of the mechanical bond on catalyst performance.

D. K., J. R., C. J. V., M. T. and D. J. conducted the experimental work. D. K. and J. N. wrote the original and revised manuscript. J. N. conceived and supervised the study.

Funding from the Deutsche Forschungsgemeinschaft DFG (project NI1273/2-2 and Heisenberg-Professorship NI1273/4-1) is gratefully acknowledged.

Conflicts of interest

There are no conflicts to declare.

Notes and references

1 C. J. Bruns and J. F. Stoddart, *The Nature of the Mechanical Bond: From Molecules to Machines*, Wiley & Sons, Hoboken, 2016.
2 (*a*) A. W. Heard, J. M. Suárez and S. M. Goldup, *Nat. Rev. Chem.*, 2022, **6**, 182–196; (*b*) C. Kwamen and J. Niemeyer, *Chem. – Eur. J.*, 2021, **27**, 175–186; (*c*) D. Sluysmans and J. F. Stoddart, *Trends Chem.*, 2019, **1**, 185–197; (*d*) D. A. Leigh, V. Marcos and M. R. Wilson, *ACS Catal.*, 2014, **4**, 4490–4497; (*e*) A. Martinez-Cuezva, A. Saura-Sanmartin, M. Alajarin and J. Berna, *ACS Catal.*, 2020, **10**, 7719–7733.
3 (*a*) J. E. Lewis, M. Galli and S. M. Goldup, *Chem. Commun.*, 2016, **52**, 298–312; (*b*) E. A. Neal and S. M. Goldup, *Chem. Commun.*, 2014, **50**, 5128–5142.
4 (*a*) V. Blanco, D. A. Leigh and V. Marcos, *Chem. Soc. Rev.*, 2015, **44**, 5341–5370; (*b*) S. F. M. van Dongen, S. Cantekin, J. A. A. W. Elemans, A. E. Rowan and R. J. M. Nolte, *Chem. Soc. Rev.*, 2014, **43**, 99–122.
5 R. Mitra and J. Niemeyer, *ChemCatChem*, 2018, **10**, 1221–1234.
6 (*a*) M. Krajnc and J. Niemeyer, *Beilstein J. Org. Chem.*, 2022, **18**, 508–523; (*b*) J. R. J. Maynard and S. M. Goldup, *Chem*, 2020, **6**, 1914–1932; (*c*) N. Pairault and J. Niemeyer, *Synlett*, 2018, 689–698; (*d*) E. M. G. Jamieson, F. Modicom and S. M. Goldup, *Chem. Soc. Rev.*, 2018, **47**, 5266–5311; (*e*) N. H. Evans, *Chem. – Eur. J.*, 2018, **24**, 3101–3112.
7 (*a*) A. W. Heard and S. M. Goldup, *Chem*, 2020, **6**, 994–1006; (*b*) M. Dommaschk, J. Echavarren, D. A. Leigh, V. Marcos and T. A. Singleton, *Angew. Chem., Int. Ed.*, 2019, **58**, 14955–14958; (*c*) Y. Cakmak, S. Erbas-Cakmak and D. A. Leigh, *J. Am. Chem. Soc.*, 2016, **138**, 1749–1751.
8 For recent examples of MIMs with nonclassical chirality, which however were not applied in catalysis, see: (*a*) S. Zhang, A. Rodríguez-Rubio, A. Saady, G. J. Tizzard and S. M. Goldup, *Chem*, 2023, **9**, 1195–1207; (*b*) N. Pairault, F. Rizzi, D. Lozano, E. M. G. Jamieson, G. J. Tizzard and S. M. Goldup, *Nat. Chem.*, 2023, **15**, 781–786; (*c*) A. Rodriguez-Rubio, A. Savoini, F. Modicom, P. Butler and S. M. Goldup, *J. Am. Chem. Soc.*, 2022, **144**, 11927–11932; (*d*) J. R. J. Maynard, P. Gallagher, D. Lozano, P. Butler and S. M. Goldup, *Nat. Chem.*, 2022, **14**, 1038–1044; (*e*) A. de Juan, D. Lozano, A. W. Heard, M. A. Jinks, J. M. Suarez, G. J. Tizzard and S. M. Goldup, *Nat. Chem.*, 2022, **14**, 179–187.
9 (*a*) M. Calles, J. Puigcerver, D. A. Alonso, M. Alajarin, A. Martinez-Cuezva and J. Berna, *Chem. Sci.*, 2020, **11**, 3629–3635; (*b*) A. Martinez-Cuezva, M. Marin-Luna, D. A. Alonso, D. Ros-Ñiguez, M. Alajarin and J. Berna, *Org. Lett.*, 2019, **21**, 5192–5196; (*c*) K. Xu, K. Nakazono and T. Takata, *Chem. Lett.*, 2016, **45**, 1274–1276; (*d*) S. Hoekman, M. O. Kitching, D. A. Leigh, M. Papmeyer and D. Roke, *J. Am. Chem. Soc.*, 2015, **137**, 7656–7659; (*e*) V. Blanco, D. A. Leigh, V. Marcos, J. A. Morales-Serna and A. L. Nussbaumer, *J. Am. Chem. Soc.*, 2014, **136**, 4905–4908; (*f*) Y. Tachibana, N. Kihara and T. Takata, *J. Am. Chem. Soc.*, 2004, **126**, 3438–3439.
10 (*a*) R. Mitra, M. Thiele, F. Octa-Smolin, M. C. Letzel and J. Niemeyer, *Chem. Commun.*, 2016, **52**, 5977–5980; (*b*) D. Jansen, J. Gramüller, F. Niemeyer, T. Schaller, M. C. Letzel, S. Grimme, H. Zhu, R. M. Gschwind and J. Niemeyer, *Chem. Sci.*, 2020, **11**, 4381–4390; (*c*) R. Mitra, H. Zhu, S. Grimme and J. Niemeyer, *Angew. Chem., Int. Ed.*, 2017, **56**, 11456–11459.
11 N. Pairault, H. Zhu, D. Jansen, A. Huber, C. G. Daniliuc, S. Grimme and J. Niemeyer, *Angew. Chem., Int. Ed.*, 2020, **59**, 5102–5107.
12 T. Ooi, M. Kameda and K. Maruoka, *J. Am. Chem. Soc.*, 1999, **121**, 6519–6520.
13 (*a*) A. Manaprasertsak, S. Tharamak, C. Schedl, A. Roller and M. Widhalm, *Molecules*, 2019, **24**, 3844; (*b*) M. Thiele, F. Octa-Smolin, S. Thölke, C. Wölper, J. Linders, C. Mayer, G. Haberhauer and J. Niemeyer, *Chem. Commun.*, 2021, **57**, 9842–9845.
14 LiOH does not significantly affect catalyst stability, as evidenced by a control experiment (see ESI† Table S1 and Fig. S36).
15 The lithium phosphate macrocycle alone does not show any catalytic activity (see ref. 11) and was thus not included in the control experiments.
16 Y.-L. Zhao, Y. Wang, X.-Q. Hu and P.-F. Xu, *Chem. Commun.*, 2013, **49**, 7555–7557.

